

Generation of lattice Wannier functions via maximum localization

Eric Cockayne¹

¹*Ceramics Division, Materials Science and Engineering Laboratory,
National Institute of Standards and Technology Gaithersburg, MD 20899-8520*

A method is presented for generating approximate lattice Wannier functions (LWF) for lattice dynamics problems, using the dynamical matrix for a supercell as input. The lattice Wannier functions fit selected phonon frequencies and eigenvectors exactly, are orthonormal, and are optimized to be maximally localized. The method easily generalizes to the case where LWF centered on more than one distinct chemical species are desired, as well as the case of solid solutions. The method is successfully applied to a one-dimensional toy model.

PACS numbers:

I. INTRODUCTION

In many lattice dynamics problems, the temperature-dependent physical properties are dominated by the low-frequency phonons. For example, the low-temperature $c_v \propto T^3$ heat capacity relationship in crystals arises from the linear dispersion of acoustic phonons near zero wavevector. A second example is the dielectric constant of dielectrics. The phonon contribution to the dielectric tensor for a crystal can be written in the form[1, 2]:

$$\kappa_{\alpha\beta} = \frac{1}{V\epsilon_0 m_0} \sum_{\omega_\mu^2 \neq 0} \frac{\overline{Z}_{\mu\alpha}^* \overline{Z}_{\mu\beta}^*}{\omega_\mu^2}, \quad (1.1)$$

where V is the unit cell volume, ϵ_0 the permittivity of free space, ω_μ the (angular) frequency of phonon μ , \overline{Z}_μ^* the electric polarization induced by phonon mode μ divided by the phonon amplitude, and m_0 an arbitrary mass that appears in the definition of \overline{Z}_μ^* . In high- κ materials, the dielectric constant is typically dominated by the contribution of low-frequency zone-center optical phonons. A third example is ferroelectric phase transitions. Typically in ferroelectrics, the ground state is largely determined by the freezing in of a particular mode which is *unstable* in the paraelectric phase[3]. To the extent that the anharmonic coupling of the instabilities of the paraelectric phase to other modes is small, the thermodynamics of the ferroelectric phase transition is determined by the properties of the unstable modes[4]. In all of the above cases, the number of degrees of freedom of the lattice dynamics problem, as it affects the temperature-dependent physical properties, can be greatly reduced by including only those degrees of freedom corresponding to the relevant phonons[5]. Furthermore, as shown by Rabe and Waghmare[4], these degrees of freedom can be spanned by a localized “lattice Wannier function” basis set. The projection of the original Hamiltonian onto the LWF yields the harmonic lattice dynamical part of an “effective Hamiltonian” in a form amenable to Monte Carlo and molecular dynamics simulations.

Despite their usefulness, the generation of LWF to date has been largely done on a case by case basis. Difficulties

in making the generation of LWF more automatic include symmetrization, localization [6], basis set completeness, and, most importantly, the band mixing or “entangled band” problem. Souza, Mazari, and Vanderbilt [7] discussed the entangled band problem for the case of electronic Wannier functions. Rabe and Caracas [8] have discussed the entangled band problem for lattice Wannier functions, and concluded that a practical solution is to impose LWF locality and to fit only the relevant (*i.e.* low frequency) parts of the phonon band(s) exactly.

In many cases, materials with the most useful properties are solid solutions. For example, temperature stability in dielectrics for microwave resonators typically requires solid solutions. Ultrahigh piezoelectric constants are found in solid solutions of $\text{Pb}[\text{Mg},\text{Zn}]_{1/3}\text{Nb}_{2/3}\text{O}_3$ with PbTiO_3 . For such systems, LWF designed for solid solutions would be useful in elucidating the physics responsible for their properties.

In this paper, an automatic procedure is given for generating LWF. As in the previous work by Rabe and Caracas, the key idea is to impose LWF locality, while fitting only the relevant part of the phonon bands exactly (although it may be desirable to include additional phonons). Furthermore, by eliminating symmetry as a consideration in generating the LWF, and using the principle of maximum localization only, the method easily generalizes to solid solutions.

II. METHOD

To generate the LWF of a solid, one begins with phonon information. Although it is desirable in principle to know the full phonon dispersion (including eigenvectors), this is not usually possible in practice. Instead, the method presented here gives approximate LWF based on phonon results for finite supercells. The required input is the eigenvalues and eigenmodes of a supercell dynamical matrix, as might be determined from first-principles (FP) calculations on the supercell, FP linear response calculations on a primitive cell, or “interpolated” results for a larger supercell using FP interatomic forces obtained for

smaller (super)cells [9].

For a supercell with N atoms, let i label the DN atomic coordinates (where D is the dimensionality of the system, and, for simplicity, the position \mathbf{r}_i and Cartesian direction coordinate $\hat{\alpha}_i$ are folded into a single label), and j the DN normal modes. Let ν_j be the j 'th dynamical matrix eigenvalue (proportional to squared frequency) and e_{ji} be the i 'th component of the (normalized) dynamical matrix eigenvector for mode j .

The LWF determination problem is to fit the ν_j and e_{ji} for a chosen subset of modes $\{u_l\} \subset \{v_j\}$, using a set of supercell-periodic functions w_{ki} , where w_{ki} is the displacement of coordinate i in basis function w_k . The w_k become the exact lattice Wannier functions in the limit of an infinite supercell.

There is no absolute criteria for which modes u_l should be included, but, for problems where the physics is dominated by the low-frequency modes, it is necessary to include those modes for which ν_j is less than some cutoff value (as discussed in Section IV, it may be desirable to include some additional modes). Note that the supercell approach, in effect, replaces continuous phonon dispersion branches with information on a discrete grid in q -space. In fact, it is this focus on individual phonons rather than phonon branches that makes it so easy to generalize to solid solutions, etc.

There is also no absolute criteria for the set of positions $\{\mathbf{r}_k\}$ on which to center the $\{w_k\}$. In many cases, certain atomic species displaced in certain Cartesian directions dominate the eigenvectors of the included modes. In such cases, it is natural to have the LWF set comprise each site $\{\mathbf{r}_k\}$ on which an atom of the given species sits, and each important direction of displacement $\hat{\alpha}_k$.

To fit the selected eigenfunctions of the original matrix exactly, one seeks (unknown) coordinates a_{lk} and w_{ki} such that $\sum_k a_{lk} w_{ki} = e_{li}$. There is no unique solution for w_{ki} because different choices of $\{a_{lk}\}$ lead to different w_{ki} . To find the "optimal" set of w_{ki} , a "localization criterion" is applied, namely, to minimize $\sum_{ki} w_{ki}^2 d_{ki}^2$. The distance metric d_{ki}^2 here is chosen to be $d_{ki}^2 = \min((r_k - r_i + \mathbf{R}_{\text{supercell}})^2)$. Other metrics may be considered, for example, "anisotropic" metrics where d_{ki}^2 is a function of $\hat{\alpha}_k$ and $\hat{\alpha}_i$ as well as the distance between the LWF centers.

Additional constraints are imposed to keep the functions w_k orthonormal and the coordinate sets a_{lk} orthonormal: $\sum_i w_{ki} w_{mi} = 1$, $k = m$; $\sum_i w_{ki} w_{mi} = 0$, $k \neq m$; $\sum_k a_{lk} a_{nk} = 1$, $l = n$; $\sum_k a_{lk} a_{nk} = 0$, $l \neq n$. The problem is then set up as a constrained minimization problem. Using Lagrange multipliers, we write:

$$\begin{aligned} f = & \sum_{ki} w_{ki}^2 d_{ki}^2 + \sum_{li} \lambda_{1li} \left(\sum_k a_{lk} w_{ki} - e_{li} \right) \\ & + \sum_k \lambda_{2kk} \left(\sum_i w_{ki} w_{ki} - 1 \right) + \sum_{k < m} \lambda_{2km} \left(\sum_i w_{ki} w_{mi} \right) \\ & + \sum_l \lambda_{3ll} \left(\sum_k a_{lk} a_{lk} - 1 \right) + \sum_{l < n} \lambda_{3ln} \left(\sum_k a_{lk} a_{nk} \right). \end{aligned}$$

One then needs to solve $\partial f / \partial w_{ki} = 0$; $\partial f / \partial a_{lk} = 0$; $\partial f / \partial \lambda_{1li} = 0$; $\partial f / \partial \lambda_{2k \leq m} = 0$; $\partial f / \partial \lambda_{3l \leq n} = 0$.

Since the above partial derivatives are nonlinear, an analytic solution does not exist in general. To extract a solution numerically, it is simpler instead to minimize the function

$$\begin{aligned} F = & 1 + \sum_{ki} (\partial f / \partial w_{ki})^2 + \sum_{lk} (\partial f / \partial a_{lk})^2 \\ & + \sum_{li} (\partial f / \partial \lambda_{li})^2 + \sum_{k \leq m} (\partial f / \partial \lambda_{2km})^2 \\ & + \sum_{l \leq n} (\partial f / \partial \lambda_{3ln})^2. \end{aligned}$$

By construction, F is minimized to 1 if and only if all partial derivatives of f are zero. There may, however, be more than one solution. A hypothesis for a reasonable starting guess for the variables is: $w_{ki} = 1$ if $\mathbf{r}_k = \mathbf{r}_i$ and $\hat{\alpha}_k = \hat{\alpha}_i$, else $w_{ki} = 0$; $a_{lk} = c_l e_{li}$ for i such that $\mathbf{r}_k = \mathbf{r}_i$ and $\hat{\alpha}_k = \hat{\alpha}_i$, with normalization constants c_l such that $\sum_k a_{lk}^2 = 1$, and all Lagrange multipliers set to zero.

After the above results are obtained, the dynamical matrix D can be replaced by D' , a reduced dynamical matrix over LWF variables. The components of D' are, in bra-ket notation:

$$D'_{km} = \langle w_k | D | w_m \rangle. \quad (2.1)$$

It is straightforward to show that

$$\langle a_l | D' | a_n \rangle = \langle e_l | D | e_n \rangle = \delta_{ln} \nu_l; \quad (2.2)$$

that is, the selected eigenvalues of the original dynamical matrices are also eigenvalues of D' , and the corresponding eigenvectors are related to the origin dynamical matrix eigenvectors through the LWF. D' also gives the harmonic lattice terms of an "effective Hamiltonian" for Monte Carlo or molecular dynamics simulations.

III. MODEL

The methods of this paper will be applied to a toy model for the lattice dynamics of a one-dimensional chain ($D = 1$). Figure 1 shows the toy linear chain model, created so as the phonon dispersion would be qualitatively similar to that often observed in ferroelectric perovskites such as BaTiO₃[10]. The chain has 4 atoms per primitive cell: an "A" or "A'" cation at each $x = \text{integer } n$, a "B" or "B'" cation at $x = n + 0.5$, and "C" anions at $x = n + 0.25$ and $x = n + 0.75$. For simplicity, all ions have mass $m = 1$, and the length of the unit cell is set to $a = 1$. Defect and solid solution phenomena are incorporated into the model through the distribution of [A,A'] and [B,B'] ions on the corresponding sublattices.

The intersite force constants are given in Table I. The force constants involving A' and B' are set to mimic certain common characteristics of perovskite solid solutions. B' is designed to be chemically very similar to B and to



FIG. 1: Primitive cell of a one-dimensional toy model for lattice dynamics.

create relatively minor perturbations of the phonon dispersion, as might occur for the substitution of one similarly sized isovalent ion for another. A' is designed so that instabilities involving A' off-centering (but not A off-centering) will occur, as happens when Li substitutes for K on the perovskite A site of $[K, Li]TaO_3$.

TABLE I: Interatomic force constants in model. For C-C interactions at distance 0.50, (A) and (B) indicate which ion is between the two "C" ions.

1	2	d_{12}	FC	1	2	d_{12}	FC
A, A'	A, A'	1.00	-37.5	B, B'	C	0.25	25
A, A'	B, B'	0.50	-15	B, B'	C	0.75	25
A	C	0.25	-15	C	C	0.50(A)	-140
A'	C	0.25	70	C	C	0.50(B)	40
A, A'	C	0.75	-15	C	C	1.00	-55
B, B'	B, B'	1.00	-107.5				
B	B, B'	2.00	28.75				
B'	B'	2.00	37.5				

Figure 2 shows the dynamical matrix eigenvalue dispersion for the "ideal" ABC_2 chain. There is a single unstable mode at $q = 0$, dominated by B participation. The instability only extends through part of the Brillouin zone (BZ). The mode with largest B participation at $q = \pi/a$ is not the lowest one, but rather the second-highest one (eigenvalue 360). Note the following analo-

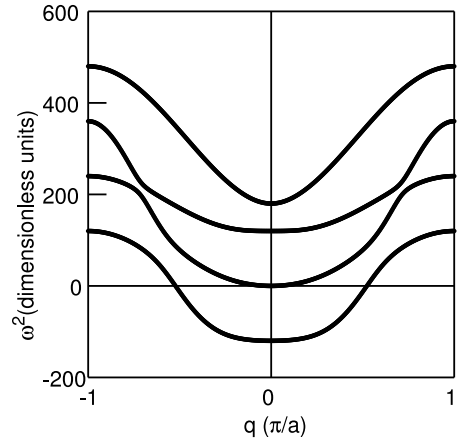


FIG. 2: Phonon dispersion for the ideal ABC_2 structure

gies with the case of $BaTiO_3$ [5, 10]: In $BaTiO_3$, there are instability branches dominated by Ti motion that do not extend throughout the entire BZ. Ti-dominated zone-boundary modes, where they occur, are not always the lowest-frequency modes at these points.

IV. RESULTS

The procedure for generating LWFs was applied to 4 structures within the toy model: (1) the "ideal" ABC_2 cell, (2) a doubled cell with composition $A_2BB'C_4$, (3) an octupled cell with composition $A_8B_4B'_4C_{16}$, with the B and B' cations arranged in the quasirandom[11] arrangement $BBBB'B'B'BB'$, and (4) an octupled cell with the composition $A_7A'B_8C_{16}$.

For a one-dimensional supercell of period Na , the BZ goes from $-\pi/(Na)$ to $\pi/(Na)$. It is possible to plot the dispersions of all the examples studied in this work in a common zone from $-\pi/(8a)$ to $\pi/(8a)$, but that yields complicated diagrams with 32 bands in each case. For simplicity, we compare instead the density of states (DOS) in each case, as shown in Figure 3.

The replacement of B with B' leads to a gap in the DOS just below $\omega^2 = 0$, a typical phenomena in period-doubling perturbations. While the DOS in the quasirandom case is similar, there is only a pseudogap, and the structure of the DOS is more complicated. The replacement of A with A' gives an additional instability branch

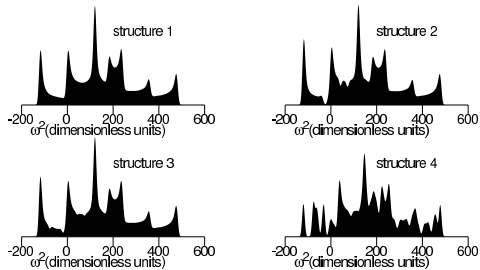


FIG. 3: Density of states of ω^2 for the configurations studied

which is nearly dispersionless. Because of coupling of A' to the other ions, the DOS is strongly perturbed over the whole frequency range, with many more singularities.

LWF were then generated for each structure. In each case, a (super)cell of length $8a$ containing 32 ions was sufficient to generate LWF that reproduced very well the phonon DOS in the low-frequency bands. Each structure had a similar set of optical low-frequency modes dominated by B, B' and with $\omega^2 < 10$. Based on the analogy of the toy model to lattice dynamics for ferroelectric transitions, where the modes of interest are the low frequency optical modes (in particular the instabilities), all supercell optical modes with $\omega^2 < 10$ were included in the LWF fits. This frequency range encompasses the additional A' -dominated branch in case (4). Based on the ions whose motion dominates the low-frequency modes, LWF centered on B and B' sites were included in all cases. One additional LWF, centered on the A' site, was included for case (4). In each case, there is a van Hove singularity in the phonon DOS at $\omega^2 \approx 360$ arising from $q = \pi/a$ -type B-dominated modes. Based on the principle that the singularities in the phonon DOS of the LWF-model should match the singularities in the original DOS as much as possible, the corresponding mode was included in each fit. Note that there is no absolute criterion why these modes should be included. As long as the number of modes fit per supercell is less than or equal to the number of LWF centers, the procedure will generate LWF that reproduce these modes, and as long

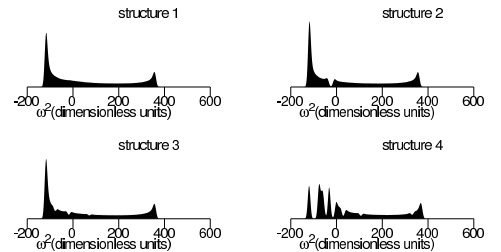


FIG. 4: Density of states of ω^2 for the effective Hamiltonians generated from the LWF for each configuration studied.

as the phonon DOS in the region that affects the physical properties is correctly reproduced, it does not matter which higher-frequency modes are included.

In each case, the function F converges to 1. Using D' and setting the interactions to zero for distances larger than the maximum distance in D' allows phonon DOS and dispersions to be calculated from the effective Hamiltonian generated for each structure. For each case, the calculated DOS are shown in Figure 4. The dispersion generated from the LWFs for ABC_2 is shown in Figure 5, and compared with the original full phonon dispersion. It reproduces the unstable part of the original model extremely well, and rises smoothly to match the A -dominated mode at $q = \pi/a$. The values for the LWF displacement of the central cations and their nearest-neighbor C anions are given in Table II.

V. DISCUSSION

The procedure for generating LWF succeeds in reproducing the low-frequency phonon DOS for all of the one-dimensional model test cases. The phonon dispersion in the Brillouin zone or reduced Brillouin zone is also reproduced in each case. The results provide strong evidence that LWF can be generated for arbitrary cation orderings in solid solutions.

In principle, the method should work in three dimen-

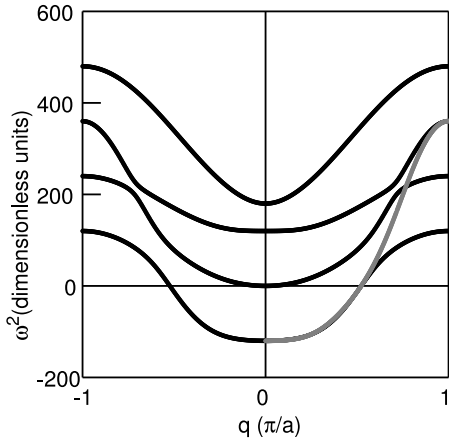


FIG. 5: (Left side) Dispersion in ω^2 of ABC_2 . (Right side) Same as left side, with the effective Hamiltonian dispersion added.

sions. Polarization of phonon eigenvectors in dimensions $D > 1$, and the corresponding possibility for multiple LWF components centered on the same ion, are technical issues to be resolved. Also, the method requires minimization of a function of $(2DNn_\mu + n_\mu n_w + n_w^2 + n_w/2 + n_\mu^2 + n_\mu/2)$ dimensions, where n_μ is the number of modes to be fit and n_w is the number of LWF centers chosen. This gives a practical limit to how large a supercell can be chosen for the fit.

In the case of the ABC_2 and $A_2BB'C_4$ structures, the LWF have "u" symmetry under reflection, and the LWF for the same species with different centers are related by translational symmetry. While these reflect the symmetry of the lattice, symmetry was not imposed by design. Rather, symmetry resulted from maximum localization. In cases (3) and (4), in fact, LWF centered on ions that are not on sites with reflection symmetry do not have any reflection symmetry, and LWF on sites that are not symmetry-related are not translationally identical (see Table II). Remarkably, even though all the phonons selected for the fit preserve the center of mass of the crystal, the individual LWFs, do not, in general conserve the center of mass. The fact that LWF centered on the same species are not in general related by symmetry means that, in the effective Hamiltonian for a solid solution, the interactions involving these LWF centers will be environment-dependent.

TABLE II: Lattice Wannier functions generated from each structure. Although the LWF extend over the unit cell, only the components for ions within distance 0.25 from the central ion are shown, as they are localized

structure	ion	position	$w_{x-0.25}$	w_x	$w_{x+0.25}$
1	B	(all)	-0.233	0.860	-0.233
2	B	(all)	-0.232	0.860	-0.232
2	B'	(all)	-0.206	0.898	-0.206
3	B	0.5	-0.231	0.859	-0.234
3	B	1.5	-0.237	0.860	-0.238
3	B	2.5	-0.234	0.859	-0.231
3	B'	3.5	-0.211	0.880	-0.226
3	B'	4.5	-0.235	0.860	-0.232
3	B'	5.5	-0.201	0.899	-0.201
3	B	6.5	-0.232	0.860	-0.235
3	B'	7.5	-0.226	0.880	-0.211
4	A'	0.0	-0.491	0.706	-0.491
4	B	0.5	-0.068	0.916	-0.234
4	B	1.5	-0.249	0.854	-0.231
4	B	2.5	-0.236	0.861	-0.211
4	B	3.5	-0.246	0.832	-0.263
4	B	4.5	-0.263	0.832	-0.246
4	B	5.5	-0.211	0.861	-0.236
4	B	6.5	-0.231	0.854	-0.249
4	B	7.5	-0.234	0.916	-0.068

Tests where the centers of the LWF were inappropriately chosen gave interesting results. For case (4), if A' centers were not included in the LWF fits, neither the density of the low-frequency states nor the phonon dispersion were correctly reproduced. For case (1), if the LWF centers were initially put on the A sites, the final solution had LWF centered on the B sites. Complete automation of the LWF procedure will require algorithms to decide which low-frequency modes are essential to the fit, where to center the LWFs, and, perhaps, which higher-frequency modes to include in order to fit singularities in the phonon DOS as much as possible.

VI. CONCLUSIONS

A simple, flexible, method has been presented for generating lattice Wannier functions and the harmonic lattice dynamical part of the corresponding effective Hamiltonians, based on constrained LWF localization. The method requires only that the user choose the sites on which to localize the LWF, and which eigenmodes of a supercell to exactly fit. When applied to various configurations of a toy 1D model, the method reproduces the desired features of the full lattice dynamics problem in each case. The procedure works equally well for simple compounds, ordered solid solutions, and disordered solid solutions.

VII. ACKNOWLEDGMENTS

I thank K. M. Rabe for useful discussions.

-
- [1] M. Born and K. Huang, “Dynamical Theory of Crystal Lattices” (Oxford: Oxford University Press), 1954.
 - [2] E. Cockayne and B. P. Burton, *Phys. Rev. B* **62**, 3735 (2000).
 - [3] M. E. Lines and A. M. Glass, *Principles and Applications of Ferroelectrics and Related Materials*, (Oxford 1977), Chap. 8.
 - [4] K. M. Rabe and U. V. Waghmare, *Phys. Rev. B* **52**, 13236 (1995).
 - [5] W. Zhong, D. Vanderbilt, and K. M. Rabe, *Phys. Rev. Lett.* **73**, 1861 (1994).
 - [6] J. Íñiguez, A. García, and J. M. Pérez-Mato, *Phys. Rev. B* **61**, 3127 (2000).
 - [7] I. Souza, N. Marzari, and D. Vanderbilt, *Phys. Rev. B* **65**, 035109 (2002).
 - [8] K. Rabe and R. Caracas, “Maximally-localized lattice Wannier functions”, http://www.tcm.phy.cam.ac.uk/~mdt26/talks/karin_rabe/karinrabe_wannier_functions.pdf (2002).
 - [9] X. Gonze, J.-C. Charlier, D. C. Allan, and M. P. Teter, *Phys. Rev. B* **50**, R13035 (1994).
 - [10] Ph. Ghosez, E. Cockayne, U. V. Waghmare and K. M. Rabe, *Phys. Rev. B* **60**, 836 (1999).
 - [11] A. Zunger, S.-H. Wei, L. G. Ferreira, and J. E. Bernard, *Phys. Rev. Lett.* **65**, 353 (1990).